# The Use of Atomic Force Microscopy for Imaging the Surfaces of Polyamide, 6

*Lidija Tušek*[1], Simona Strnad[1], Karin Stana-Kleinschek[1], Volker Ribitsch[2], Carsten Werner[3]*

[1]University of Maribor, Smetanova 17, SI-2000 Maribor, Slovenia
[2]Karl-Franzens Universiy Graz, Universitätsplatz 3, A-8010 Graz, Austria
[3]Institute of Polymer Research, Hohe Straße 6, D-01069 Dresden, Germany

**Summary:** The surface morphologies of PA 6 resulting from the use of various processing methods were studied by tapping mode atomic force microscopy. Three PA 6 samples: (1) a thin film, spin coated on a silicon wafer, (2) a freestanding film, i.e. a foil and (3) a monofilament, show definite morphological differences revealing typical supramolecular structures. The thin film having thickness of app. 35 nm is a good example of the initial step of spherulite formation where the sheaf development is still prominent. In an area of 100 $\mu m^2$ 1-4 spherulites can be detected which are typical of crystallization from the solution. The annealing (vacuum, 195°C, 3.5h) causes additional crystallization, which leads to a radial co-ordination and enlargement of spherulites to app. 50% in diameter and up to 40% in height. The morphology of foil (thickness of 100 μm) can be interpreted as a system of spherulites formed from the melt, and a typical fibrillar structure is observed on the surface of monofilament.

## Introduction

Polyamides are characterized by their good thermal stability, flexibility, and mechanical properties.[1] They are tough, strong, and abrasion resistant. PA 6 is therefore one of the most important materials used for synthetic textile fibres, tapes, cable insulation and in packaging.[2] In nearly all applications, these materials are melt processed. The properties of the manufactured articles are then largely determined by their supramolecular structure and the arrangement of the crystals grown from the melt during processing. It is agreed that the basic unit of polymer crystallisation is the lamellar crystal formed by chain folding.[3,4] When polymers are crystallized from the melt the lamellar crystals usually form aggregates of one form or another. The most common such aggregate is spherulite. An oriented microfibrillar structure of fibres is, according to Peterlin, the result of lamellas deformation process during the drawing of the spun fibre.[5] A microfibrillar structure of highly drawn films was also observed on the surface as a result of the deformation of the spherulites.[6]

 CCC 1022-1360/00/$ 17.50+.50/0

Scanning electron microscopy (SEM) is the most widely used method for the sub-micron imaging of surfaces including polymers, but lately the atomic force microscope (AFM) can be used as an alternative.[3] The AFM is one of the most modern types of microscopy and a detailed description of the AFM operational principle can be found in the literature [8-12] and also several tutorials are available on the Internet.[13-15] A comprehensive review of the characterisation of polymer surfaces using AFM was given by Magonov and Reneker.[15] Recently even fibres have been studied using AFM.[17-22]

Reports concerning PA 6 are very rare although the use of AFM for polymer characterisation is increasingly popular. Ferreiro *et al.* observed shear banding in PA 6 films.[22] No reference on AFM study of PA 6 fibres or PA 6 supported thin films was found in the literature.

The aim of this work was to study the surface morphologies of PA 6 resulting from the use of various processing methods. Three PA 6 samples made out from the same raw polymer: (1) a thin film, spin coated on a silicon wafer, (2) a freestanding film, i.e. foil and (3) a monofilament were chosen for this study. Our attention focused on scans with scan sizes between (2×2 $\mu m^2$) and (20×20 $\mu m^2$) without attempting to obtain molecular resolution. In this range, characteristic differences between the samples are revealed. The surface morphology of PA 6 as observed by AFM is of special interest for our research work on the surface and adsorption properties of differently structured PA 6.

## Experimental

### Materials

The material used for experiments was polyamide 6 supplied by BASF in the form of *a monofilament* with a diameter of 200 μm (draw ratio of 5.3) and a 100 μm thick freestanding film, i.e. *a foil*. Pieces of foil were cut to app. 10×5 $cm^2$ and the monofilament was wound on stainless steel cylinders (restrained - to keep the same orientation). Samples prepared in this way were cleaned with distilled water (3 hours, 40°C), rinsed well and dried in air overnight. The next day additional cleaning with ethanol for 3 hours at 40°C was carried out and followed by rinsing and drying in air overnight prior to AFM analysis.

*A thin film* of PA 6 was prepared with a spin coating of PA 6 solution over a silicon wafer. A piece of cleaned foil was dissolved in 1,1,1,3,3,3-hexafluor-2-propanol to give 0.25% solution and the next day filtrated using a glass filter B2. Several pieces of silicon

wafer (1×1 $cm^2$) were exposed to UV light source for 1 hour, put in a glass vessel and exposed to the vapour from a drop of 1,1,1,3,3,3-hexamethyldisilazane over night in order to achieve sufficient hydrophobicity of silicon surface before coating. The parameters for spin coating using the RC 8 Spin Coater (Karl Suss Technique, Munich, Germany) were as follows: time of 30 sec, speed of 2000 rpm, and acceleration of 1500 rpm/s. Spin coated films were dried in vacuum at 40°C overnight.

The thickness of the film was determined to be 35 ± 2 nm using the M44 H-VASE Ellipsometer (J.A. Woollam Co., Nebraska, USA).

**Method - AFM**

A Dimension 3100 NanoScope scanning probe microscope (Digital Instruments, Santa Barbara, USA) was used to observe the surface topography. A tapping mode, which measures topography by tapping the surface with an oscillating probe tip, was used as a scanning mode. A single beam silicon tip (cantilever length 228 μm, spring constant 1.5-6.3 N/m, resonant frequency 63-100 kHz, nominal tip radius of curvature less than 5 nm) supplied by Nanosensors (Wetzlar-Blankenfeld, Germany) was used for all measurements.

The sample roughness was characterised by three parameters: (a) Z range which gives the value in nm between the lowest and the highest point within the given area, (b) the standard deviation of the Z values within the given area, also known as RMS and (c) the mean roughness (Ra) which is the mean value of the surface relative to the centre plane. [23]

## Results and discussion

The AFM images in Figure 1 show the most typical morphological patterns on the surface of the film that was crystallised from diluted solution. Four spherulites marked A-D are detected in a scan area of 10×10 $\mu m^2$ in Figure 1a. The spherulite A has a diameter of app. 600 nm and is in the initial stage of formation showing dominant nuclei with almost no branching of fibrils. Spherulites B and C have been nucleated so closely together that their fibrils are mingled in the region of mutual contact. Two central nuclei are raised to different heights; the highest point of spherulite B lies at 12 nm and of spherulite C at 8 nm, respectively. The spherulite D in Figure 1a and spherulites in Figures 1b and 1c are the most typical and they can be found all over this sample.

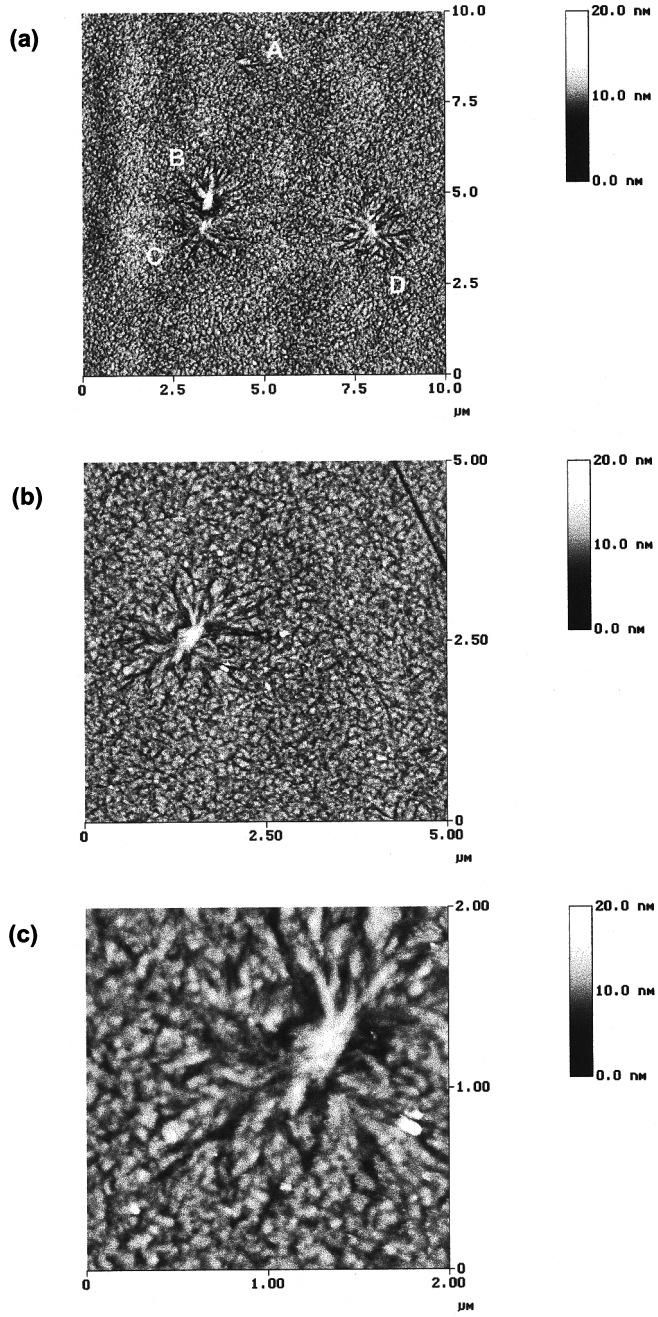


Figure 1. AFM tapping mode height images of a spin coated film on a silicon wafer in scan areas of (a) 10×10 $\mu m^2$, (b) 5×5 $\mu m^2$ and (c) 2×2 $\mu m^2$.

They are not fully-grown and the sheaf development is prominent. The fibrils spread out from a central nucleus and branch out to 1.5 - 2.5 μm in maximum diameter and up to 12 nm in height. The surrounding of spherulites has a structure formed of grains having 20-200 nm in diameter and up to 5 nm in height.

The annealing of spin-coated films at 195°C for 3.5 hrs in a vacuum causes further crystallisation. As Figure 2 shows, the spherulites are enlarged and developed into radial symmetric structural entities. The diameters of spherulites are 1.8 - 2.6 μm and are up to 14 nm in height. In addition, the grainy surrounding structure is more prominent with enlarged grains having 50-300 nm in diameter and up to 7 nm in height.

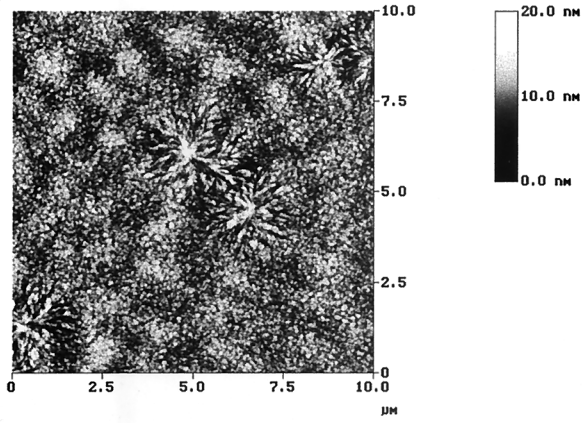


Figure 2. AFM tapping mode images of annealed spin coated film on a silicon wafer in a scan area of (a) 10×10 $\mu m^2$.

As shown in Table 1 roughness analysis also detects the effect of additional crystallisation. The raw spin-coated film as imaged in Figure 1a gives the Z value (the distance between the lowest and the highest points within the given area) of 16 nm, the RMS (the standard deviation of the Z values within the given area) of 1.3 nm and a mean roughness Ra of 1.0 nm. Due to annealing the Z range calculated from Figure 2 is increased by 25% (20 nm), RMS by 54% (2 nm) and Ra by 60% (1.6 nm), respectively. The annealing, besides spherulites, also influences the surrounding grainy texture which can be seen by comparing the results of roughness analysis on a small sector (1 × 1 $\mu m^2$) where no spherulites are present. The Z range of grainy structure is increased from 10 to 16 nm (60%), RMS from 1.2 to 1.8 nm (50%), and Ra from 0.9 to 1.4 (55%),

respectively.

Table 1. Roughness analysis of spin-coated films before and after annealing.

| Scan range | Raw | | | Annealed | | |
|---|---|---|---|---|---|---|
| | Z | RMS | Ra | Z | RMS | Ra |
| | nm | nm | nm | nm | nm | nm |
| 10×10 $\mu m^2$ | 16 | 1.3 | 1.0 | 20 | 2.0 | 1.6 |
| 1×1 $\mu m^2$ (grainy surroundings) | 10 | 1.2 | 0.9 | 16 | 1.8 | 1.4 |

Figure 3 shows the AFM tapping mode images of the PA 6 foil. Figure 3a shows the typical surface morphology of a sample on a bigger scale and figure 3b gives a close up of the central part of the first image.

The brighter regions in Figure 3 represent the higher and the darker regions the lower parts of the sample with a height variation of 100 nm (scan size of 20×20 $\mu m^2$) and 20 nm (scan size of 5×5 $\mu m^2$), respectively. The morphology of the foils can be approximated as a system of banded spherulites, which are typical of melt-crystallisation. As the spherulites grow larger and become more numerous, spherical development is gradually interrupted because of mutual contact giving an assemblage composed of various shaped polygons. This phase of growth is often referred to as primary crystallisation.[24] Next further, or secondary, crystallisation proceeds within each spherulite, transforming a portion of the remaining amorphous macromolecules trapped between the crystals. The entire assemblage in Figure 3b, therefore, resembles a jigsaw puzzle composed of polygons of various shapes. Beams coming out of a spherulite centre, which are blurred, are formed of grains partially merging with each other. The size of the grains is in the 20 - 250 nm range and, in a number of areas on the surface, linear sequences of grains can be distinguished. These grains are up to 10 nm high which is comparable to the height of the spherulites in Figure 1 (up to 12 nm). The inter-spherulitic boundaries represent discontinuities, which impart a grainy texture best seen from the 3D plot in Figure 4.

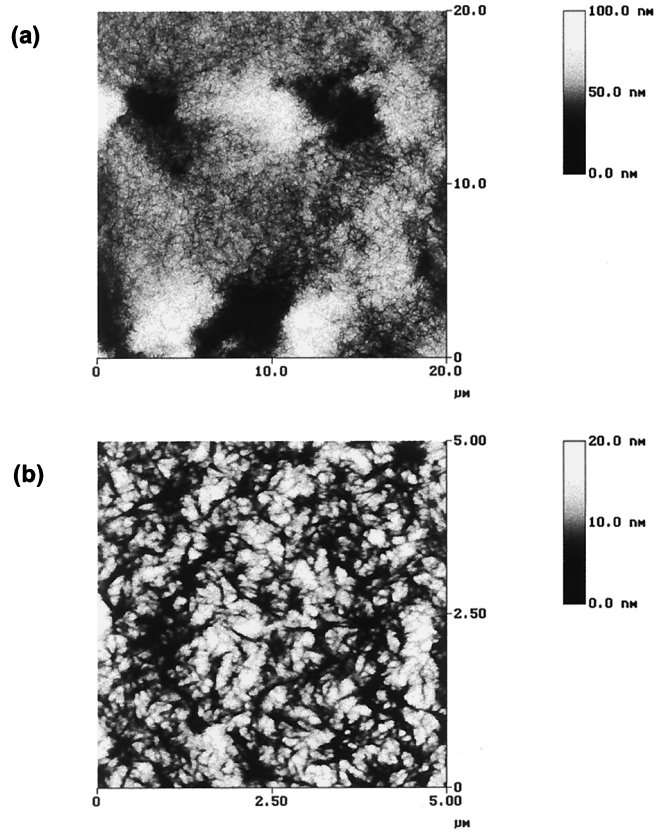


Figure 3. AFM tapping mode images of PA 6 melt-crystallised foil on a scan area of (a) 20×20 $\mu m^2$ and (b) 5×5 $\mu m^2$ – a close up of the central part of Figure 3a.

The granular nanostructure of spherulites has also been observed in the AFM images of other polymers such as polyethylene, polyester and polyurethane.[15, 25] Based on X-ray diffraction data, Terrill *et al.* showed that, during the cooling of crystallizable polymers from melt, the SAXS pattern (which is relevant to formation of nanoscale ordering) appears before the WAXS (wide-angle X-ray scattering) pattern (which is relevant to molecular-scale ordering).[26] These results and those presented by Magonov and Godovsky[27] suggest that individual nanoscale grains can be considered as elementary building blocks in the crystalline architecture of polymers. Each grain or block may have a more ordered interior and less ordered exterior depending on the particular polymerisation and crystallization condition. It was suggested that crystalline

morphology could be developed via the one-dimensional assembling of grains into the fibrils and two-dimensional assembling of grains into lamella.[27] The granular nanostructure of spherulites has also been observed in the AFM images of other polymers such as polyethylene, polyester and polyurethane.[15, 28] Based on X-ray diffraction data, Terrill *et al.* showed that, during the cooling of crystallizable polymers from melt, the SAXS pattern (which is relevant to formation of nanoscale ordering) appears before the WAXS (wide-angle X-ray scattering) pattern (which is relevant to molecular-scale ordering).[29] These results and those presented by Magonov and Godovsky[30] suggest that individual nanoscale grains can be considered as elementary building blocks in the crystalline architecture of polymers. Each grain or block may have a more ordered interior and less ordered exterior depending on the particular polymerisation and crystallization condition. It was suggested that crystalline morphology could be developed via the one-dimensional assembling of grains into the fibrils and two-dimensional assembling of grains into lamella.[27]

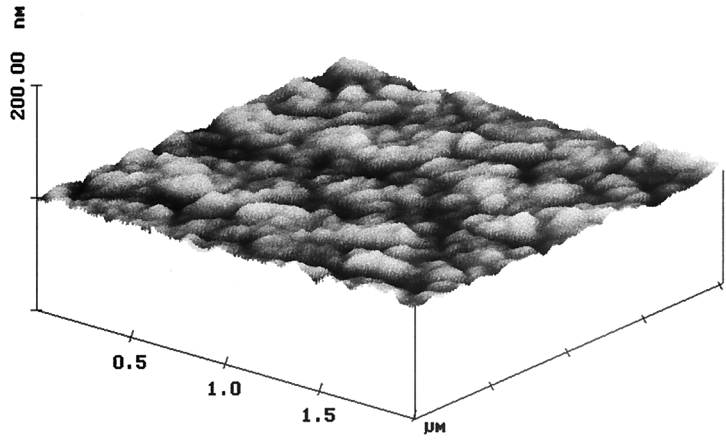


Figure 4. The 3D plot of PA 6 foil on a scan size of 2×2 $\mu m^2$.

Figure 5 shows 3D plot of filament on a 20×20 $\mu m^2$ scan size, from which it is evident that the surface of the round filament is curved, but the curvature is exaggerated. The x-y

plane is extending on a 20×20 $\mu m^2$ but the z-axis, which represents the height, comprises only 1 µm. Since the diameter of the filament is 200 µm, the height of the real arc on a 20×20 $\mu m^2$ scan size is app. 500 nm. The curvature should be taken into consideration when round samples are imaged, because the surface structure can be masked by it. The fibrils rising from the lowest regions are only up to 70 nm high, and on a bigger scale, they don't produce enough contrast to be seen, therefore typical black bands (low regions) on both sides of the image are due to curvature (Figure 6a).

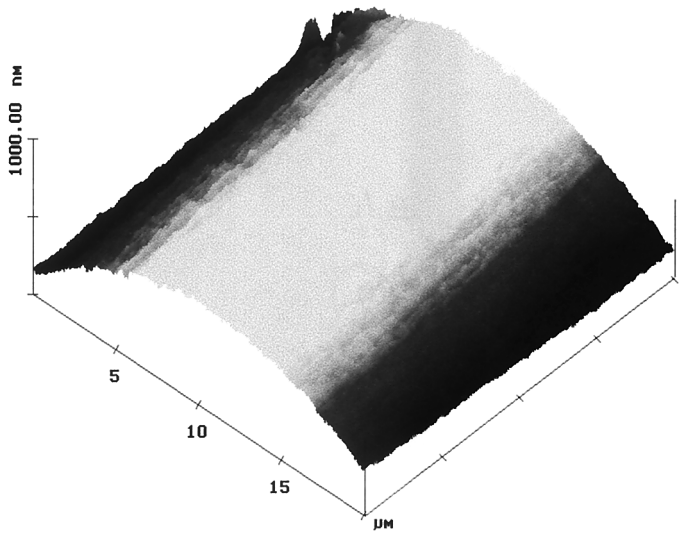


Figure 5. The 3D plot of PA 6 monofilament on a scan size of 20×20 $\mu m^2$.

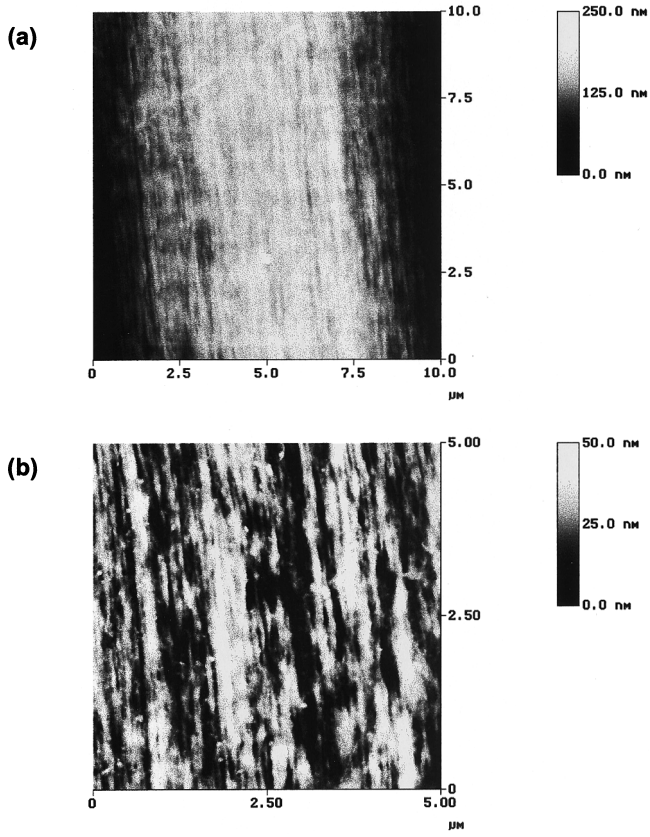


Figure 6. AFM tapping mode images of monofilament on a scan area of (a) 10×10 $\mu m^2$ and (b) 5×5 $\mu m^2$.

On a smaller scan size such as 5×5 $\mu m^2$ in Figure 6b or 2×2 $\mu m^2$ in Figure 7 a typical fibrillar structure of monofilament is observed. The smallest detectable fibrils are in the range of 10 nm in width. They are congregated in bigger fibril bundles being up to 1-2 μm in diameter. Cavities and niches vary in width (30-200 nm) and shape (round or oblong). They are oriented in the direction of the fibre axis. The surface of the filament is less furrowed in the direction of the fibre axis; the difference in height between the highest and the lowest regions alongside is only up to 30 nm and transversely up to 70 nm.

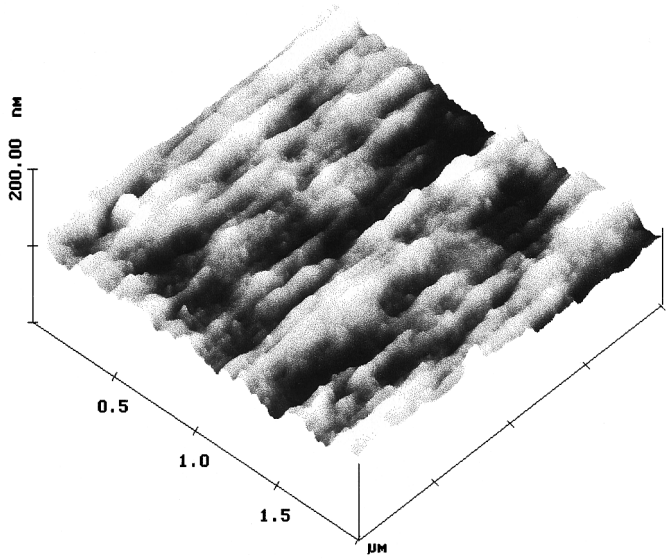


Figure 7. The 3D plot of PA 6 monofilament on a scan size of 2×2 $\mu m^2$.

## Conclusions

Atomic force microscopy (AFM) is a worthy tool for investigating the surface morphology of polymers, especially because almost no sample preparation is needed before imaging. It has been shown that AFM reveals differences between the surface morphologies of PA 6 resulting from the use of various processing methods.

A thin film on a silicon wafer shows isolated spherulites having a diameter of 1-2.5 µm and a height of up to 12 nm, which are formed by crystallisation from diluted solution. The additional crystallisation caused by annealing can be evaluated using roughness analysis or by determining any enlargement of the spherulites using section analysis.

The surface morphology of a freestanding film (i.e. foil) can be interpreted as a system of banded spherulites formed from melt. The typical grainy structure of polygons having up to 250 nm in maximum diameter and up to 10 nm in height was observed.

The PA 6 monofilament shows a typical fibrillar structure with fibrils as small as 10 nm and fibril bundles having up to 1-2 µm in diameter. The curvature of the round filament

should be taken into consideration when discussing the surface morphology of round samples.

[1] N.G. McCrum, C.P. Buckley, C.B. Bucknall, "*Principles of Polymer Engineering*", Oxford University Press, Oxford **1997**.
[2] J.H. Briston, L.L. Katan, "*Plastics Films*", Longman Scientific & Technical, Hong Kong **1986**.
[3] R.W. Cahn, P. Haasen, E.J. Kramer, in: "*Materials Science and Technology, Vol. 12: Structure and Properties of Polymers*", ed., E. L. Thomas, VCH Publishers, Weinheim, New York, Basel, Cambridge, Tokyo **1993**.
[4] B. Wunderlich, "*Macromolecular Physics, Vol. 1: Crystal Structure, Morphology, Defects*", Academic Press, New York, London **1973**.
[5] A. Peterlin, *J. Polymer Sci. Part C* **1965**, *9*, 61.
[6] R.J. Samuels, *Structured Polymer Properties, "The Indentificarion, Interpretation, and Application of Crystalline Polymer Structure"*, Wiley, New York **1974**.
[7] G. Binnig, H. Rohrer, Ch. Gerber, E. Weibel, *Phys. Rev. Lett.* **1983**, *50*, 120.
[8] G. Binnig, C.F. Quate, C.H. Gerber, *Phys. Rev. Lett.* **1986**, *56*, 930.
[9] D. Rugar,. P. Hansma, *Physics Today*, **1990**, *42*, 23.
[10] R. Wiesendanger, "*Scanning Probe Microscopy and Spectroscopy. Methods and Application*", Cambridge University Press, Cambridge **1994**.
[11] C. Bai, J. Li, Z. Lin, J. Tang, C. Wang, *Surf. Interface Anal.* **1999**, *28*, 44.
[12] NC State University, Basic principles of scanned probe microscopy, http://spm.aif.ncsu.edu/tutorial.htm.
[13] Digital Instruments, Application notes, http://www.di.com/app_notes/full_appnotes.htm.
[14] ThermoMicroscopes, Practical Guide to Scanning Probe Microscopy, http://www.thermomicro.com/spmguide/contents.htm.
[15] S.N. Magonov, D. Reneker, *Annu. Rev. Mater. Sci.* **1997**, *27*, 175.
[16] A. Wawkuschewski, H.J. Cantow, S.N. Magonov, J.D. Hewes, M.A. Kocur, *Acta Polymer.* **1995**, *46*, 168.
[17] T.C. Pesacreta, L.C. Carlson, B.A. Triplett, *Planta* **1997**, *202*, 435.
[18] J. Hautojärvi and A Leijala, *J. Appl. Polym. Sci.* **1999**, *74*, 1242.
[19] T.L Phillips, T.J Horr, M.G. Huson, P.S.Turner, R.A Shanks, Textile Res J 1995, *65*, 445.
[20] S. Rebouillat, J.-B. Donnet, T. K. Wang, Polymer 1997, *38*, 2245.
[21] S. Putthanarat , N. Stribeck, S.A. Fossey, R.K. Eby, W.W. Adams, *Polymer* **2000**, *41*, 7735.
[22] V. Ferreiro, Y. Pennec, R. Seguela, G. Coulon, *Polymer* **2000**, *41*, 1561.
[23] NanoScope Command Reference Manual, Version 4.42, Digital Instruments, 1999.
[24] L.E. Alexander, "*X-Ray Diffraction Methods in Polymer Science*", R.E. Krieger Publishing Company, Huntington **1979**.
[25] R.B. Boyd, J.P.S. Badyal, Adv. Mat. **1997**, *9*, 895.
[26] N.J. Terrill, P.A. Fairclough, E. Towns-Andrews, B. U. Komanschek, R. J. Young, A. J. Ryan, *Polymer* **1998**, *39*, 2381.
[27] S. Magonov, Y. Godovsky, *American laboratory* **1999**, *31*, 52.
[28] R.B. Boyd, J.P.S. Badyal, Adv. Mat. **1997**, *9*, 895.
[29] N.J. Terrill, P.A. Fairclough, E. Towns-Andrews, B. U. Komanschek, R. J. Young, A. J. Ryan, *Polymer* **1998**, *39*, 2381.
[30] S. Magonov, Y. Godovsky, *American laboratory* **1999**, *31*, 52.